

## REVIEW

## Taking tumour budding to the next frontier — a post International Tumour Budding Consensus Conference (ITBCC) 2016 review

Linda Studer,<sup>1,2,3</sup> Annika Blank,<sup>1</sup> John-Melle Bokhorst,<sup>4</sup> Iris D Nagtegaal,<sup>4</sup> Inti Zlobec,<sup>1</sup> Alessandro Lugli,<sup>1</sup> Andreas Fischer<sup>2,3</sup> & Heather Dawson<sup>1</sup> 

<sup>1</sup>Institute of Pathology, University of Bern, Bern, <sup>2</sup>iCoSys Institute, University of Applied Sciences and Arts Western Switzerland, HES-SO/Fribourg, Fribourg, <sup>3</sup>DIVA Research Group, University of Fribourg, Fribourg, Switzerland, and <sup>4</sup>Department of Pathology, RIMLS/RIHS Radboud University Medical Centre, Nijmegen, The Netherlands

---

Studer L, Blank A, Bokhorst J-M, Nagtegaal I D, Zlobec I, Lugli A, Fischer A & Dawson H. (2021) *Histopathology* 78, 476–484. <https://doi.org/10.1111/his.14267>

### Taking tumour budding to the next frontier — a post International Tumour Budding Consensus Conference (ITBCC) 2016 review

Tumour budding in colorectal cancer, defined as single tumour cells or small clusters containing four or fewer tumour cells, is a robust and independent biomarker of aggressive tumour biology. On the basis of published data in the literature, the evidence is certainly in favour of reporting tumour budding in routine practice. One important aspect of implementing tumour budding has been to establish a standardised and evidence-based scoring method, as was recommended by the International Tumour Budding Consensus Conference (ITBCC) in 2016. Further

developments have aimed at establishing methods for automated tumour budding assessment. A digital approach to scoring tumour buds has great potential to assist in performing an objective budding count but, like the manual consensus method, must be validated and standardised. The aim of the present review is to present general considerations behind the ITBCC scoring method, and a broad overview of the current situation and challenges regarding automated tumour budding detection methods.

Keywords: colorectal cancer, digital pathology, ITBCC, tumour budding

---

### Introduction

Tumour budding (single tumour cells or small clusters of four or fewer tumour cells<sup>1</sup>) is a sign of dissociated tumour spread, and has emerged as an independent prognostic factor not only for colorectal cancer (CRC), in which it has been most extensively studied, but also for carcinomas of other organs.<sup>2,3</sup> The prognostic significance of tumour budding in solid cancers has been the topic of many reviews and meta-analyses.<sup>4–9</sup>

Over time, many different methods have been used to assess tumour budding.<sup>5,7</sup> These differ in terms of staining [haematoxylin and eosin (H&E) versus immunohistochemical], quantification versus subjective impression, field size, and area of assessment (hotspot versus average among several fields). Despite the different methods used in studies, tumour budding retains its relevant associations with clinicopathological parameters, underlining its strong prognostic power.

However, in the era of personalised healthcare, a robust prognostic and/or predictive biomarker should be hypothesis-driven, reproducible, and cost-effective. Two important tools for achieving these goals are standardisation and automation. The former can be

Address for correspondence: Heather Dawson, MD, Institute of Pathology, University of Bern, Murtenstrasse 31, CH-3008 Bern, Switzerland. e-mail: heather.dawson@pathology.unibe.ch

achieved by establishing an evidence-based consensus. Therefore, the goal of the 2016 International Tumour Budding Consensus Conference (ITBCC) was to provide a set of evidence-based guidelines and a proposed scoring method for tumour budding in CRC, which represent a baseline starting point for implementing the assessment of tumour budding in routine practice and can be used for clinical trials and meta-analyses.

A further step, such as that taken by the Immunoscore Consortium, would be to develop a robust digital pathology approach<sup>10</sup> for the assessment of tumour budding. Advances in image analysis will undoubtedly facilitate the assessment of tumour budding in the future, but many hurdles must be overcome before automated detection can be reliably applied in daily diagnostic practice. Therefore, the aim of the present review is to give an overview of the ITBCC consensus method and outline recent advances and current challenges regarding automated tumour budding assessment.

### General considerations regarding the ITBCC 2016 scoring system

The ITBCC was initiated because of the reasoning that an evidence-based standardised set of recommendations would facilitate more widespread reporting of tumour budding and its implementation to guide patient management. Prior to and at the conference, a comprehensive literature review on published tumour budding studies was undertaken, forming the basis of the recommendations.<sup>1</sup> The selected scoring system is based on the method as proposed by Ueno in 2004 (0.785-mm<sup>2</sup> hotspot method with assessment at  $\times 20$  and H&E staining at the invasive tumour front, three-tier system). One of the main reasons for adopting this method was that it had been used to generate the most outcome-based data demonstrating tumour budding as an adverse prognostic factor.

A three-tier system (Bd1, Bd2, and Bd3) was favoured over a two-tier system (low versus high) because the three-tier system can be used for reporting tumour budding in different clinical scenarios with varying endpoints. For instance, in pT1 CRC, the issue at stake is the risk of nodal metastases, so a different scale must be used than for stage II tumours, for which the relevant clinical endpoints are recurrence-free survival and overall survival. Hence, in pT1 CRC, Bd2 and Bd3 tumours are both at higher risk for nodal metastases, whereas, in stage

II tumours, only Bd3 is considered to be a risk factor for poor survival.

In addition to budding category, which is practical for clinical decision-making, it is also recommended to report the absolute number of tumour buds, as the biological behaviour of tumour budding is that of a continuous variable, and a numerical value will enable more precise risk stratification. This is especially the case for the Bd3 category, which has no upper limit. Also, reporting the absolute budding count conveys whether a tumour lies within a borderline area. For instance, a tumour with nine buds (Bd2) is biologically similar to a tumour with 10 buds (Bd3), but falls into a different risk category. Another issue is that the present three-tier system does not have a designated category for tumours with no buds at all (these fall under the Bd1 category), and this is only clear when the absolute number of buds is reported. In any case, it must be emphasised that tumour budding must not be a 'stand-alone' clinical decision-maker, but must be taken into account with other histopathological and clinical risk factors in a multidisciplinary setting (e.g. tumour rounds).

The field diameter must also be considered when tumour buds are quantified, as field areas can vary considerably depending on the microscope. For example, a 20-mm field number diameter eyepiece corresponds to an area of 0.785 mm<sup>2</sup> at  $\times 20$ , whereas this area is 1.227 mm<sup>2</sup> with a 25-mm eyepiece (+56%). As a considerably higher number of buds will be counted with the 25-mm eyepiece, a normalisation factor will artificially correct this difference. As the majority of the data and the adopted category cut-offs were derived from a 0.785-mm<sup>2</sup> hotspot, it was decided to recommend reporting tumour budding normalised to this area. Many microscopes in the western world have a 22-mm field number diameter (0.95 mm<sup>2</sup> at  $\times 20$ ), so the number of counted buds must be divided by the normalisation factor 1.21 prior to reporting.

As the majority of outcome-based data were derived from budding assessment on H&E-stained slides, the assessment of tumour budding on H&E-stained slides was recommended. However, tumour buds may sometimes be difficult to identify, e.g. in the case of a brisk inflammatory infiltrate or peritumoral desmoplastic stromal reaction (Figure 1). In such cases, a cytokeratin stain may be used to confirm the suspicion of tumour budding, but the count should be performed on the H&E-stained slide.

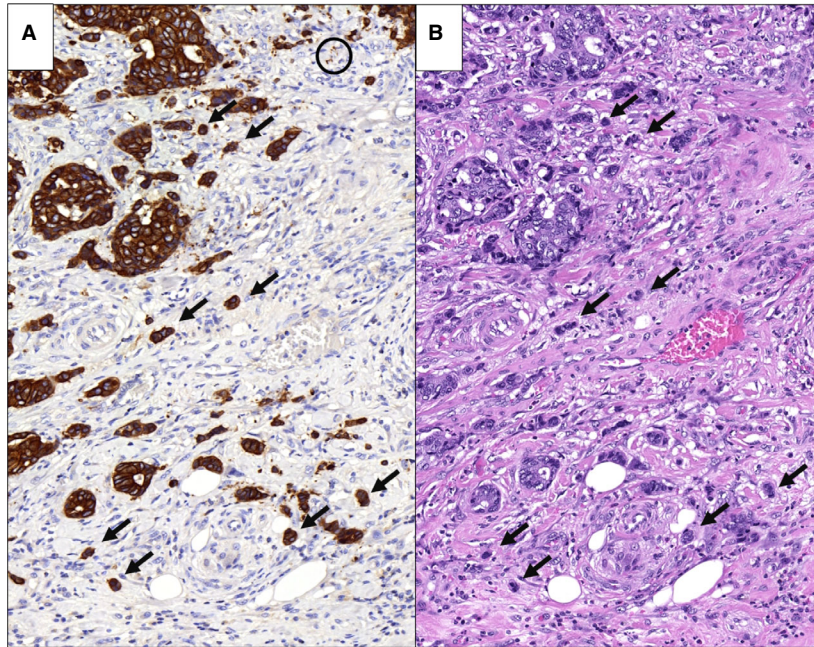


**Figure 1.** Example of a colorectal cancer with high-grade tumour budding (selected tumour buds are marked with arrows). **A**, Pan-cytokeratin stain. **B**, Corresponding haematoxylin and eosin stain. With keratin stains, both the human eye and digital solutions will detect a higher number of tumour buds and reliably distinguish buds from inflammatory and reactive stromal cells. However, keratin stains will also stain fragmented cells and debris (A, circle), which should not be regarded as tumour buds.

### Automated scoring of tumour buds—where do we stand?

Scoring tumour budding according to the ITBCC method requires a bud count in a certain area, and this process, by its nature, requires time and training, and is subject to interobserver and intraobserver variation.<sup>11,12</sup> Interobserver variation in tumour budding assessment can be suboptimal, and depends on multiple factors, such as training and experience.<sup>13,14</sup> Therefore, numerous efforts have been made to automate tumour budding assessment. As with the proposed manual assessment methods, many different options for automatic tumour budding detection have been investigated, making comparisons difficult.

To the best of our knowledge, there are 12 publications that have proposed and evaluated different methods and levels of automation (Table 1). The vast majority require certain manual steps, which usually involve the selection of a region of interest (ROI) or the exclusion of unwanted areas, such as necrotic tissue. To date, only one proposed system has an end-to-end solution.<sup>15</sup>

Most semi-automatic tumour scoring methods have been developed with immunohistochemically stained

slides,<sup>11,12,15–21</sup> in some cases with immunofluorescent staining.<sup>20,22,23</sup> Only one detection system has been proposed for H&E-stained slides.<sup>24</sup>

As tumour budding is best described in CRC, it is not surprising that most of the methods have also been developed with CRC tissue.<sup>11,12,15,17,18,20,21,23,24</sup> However, automation attempts have also been evaluated for early-stage oral squamous cell carcinoma,<sup>16</sup> muscle-invasive bladder cancer,<sup>22</sup> and breast tumours.<sup>19</sup>

Automation also highly facilitates the analysis of tumour budding in larger tissue areas, as well as the comparison of different tissue areas, such as intratumoural budding versus budding at the tumour front. This will also help to determine which areas are best for counting tumour budding in different cancer types, as not all studies have found that counting at the invasive front leads to significant associations with relevant clinical endpoints.<sup>12,22</sup>

Both commercially available software<sup>16,17,20,22,23</sup> and open-source<sup>18,19</sup> image analysis software have been used to investigate automated tumour bud detection. Most approaches use a combination of classic image analysis operations, such as binarisation and colour deconvolution, with a machine learning algorithm.<sup>12,20–24</sup> However, automated tumour bud

**Table 1.** Overview of published works on automated tumour budding assessment

| Reference                            | Year | Cancer type                              | Nos. of patients, slides, and images | Staining           | TB definition (number of cells) | Investigated tissue area                                      | Image analysis methods   | Method availability   | Endpoints   |
|--------------------------------------|------|--|--------------------------------------|--------------------|---------------------------------|---|--|---|---|
| Caie <i>et al.</i> <sup>20</sup>     | 2014 | CRC (Dukes A, B, C)                      | 50 patients                          | Immunofluorescence | 1–5                             | Stroma at invasive front                                      | Manual selection of ROI<br>Machine learning for tumour object identification and segmentation<br>TBs identified on the basis of the number of nuclei               | Commercial software (Definiens)                                       | Risk stratification and correlation with survival   |
| Pedersen <i>et al.</i> <sup>16</sup> | 2017 | Early-stage oral squamous cell carcinoma | 222 patients                         | IHC                | 1–5                             | Invasive front  | Manual exclusion of necrotic and salivary gland areas<br>TBs identified on the basis of area   | Commercial software (Visiopharm)                                      | Correlation with survival and occult LNM  |
| Bokhorst <i>et al.</i> <sup>24</sup> | 2018 | CRC                                      | 60 patients                          | H&E                | 1–4                             | 0.785-mm <sup>2</sup> hotspots (ITBCC 2016)                   | Manual selection of hotspots<br>Deep learning to detect tumour objects<br>TBs identified on the basis of size  | Algorithm details are provided  | Rate of detection of individual tumour buds (F1 score = 36%, sensitivity = 72%) and interobserver variability |
| Weis <i>et al.</i> <sup>12</sup>     | 2018 | CRC                                      | 20 patients                          | IHC                | 1–5                             | TMA cores and WSI   | Manual selection of ROI<br>Objects of interest are selected on the basis of size<br>TBs identified by the use of deep learning                                     | Algorithm details and some code are provided (programmed with MATLAB) | Bud detection and correlation with clinical outcome (nodal status)  |
| Jepsen <i>et al.</i> <sup>17</sup>   | 2018 | CRC (pT1 and pT2)                        | 126 patients                         | IHC                | 1–4                             | 0.238-mm <sup>2</sup> circular hotspots at the invasive front | A hotspot suggested by the algorithm needs to be approved by pathologists<br>TBs identified on the basis of size, the number of nuclei, and morphological features | Commercial software (Visiopharm)                                      | Hotspot and tumour bud detection, interobserver agreement, and association of tumour budding with LNM         |

**Table 1.** (Continued)

| Reference                      | Year | Cancer type                    | Nos. of patients, slides, and images      | Staining           | TB definition (number of cells) | Investigated tissue area   | Image analysis methods   | Method availability  | Endpoints  |
|--------------------------------|------|--------------------------------|---|--------------------|---------------------------------|--|--|--|--|
| Takamatsu et al. <sup>18</sup> | 2018 | CRC (T1)                       | 463 patients                              | IHC                | 1–4                             | Hotspots of 0.95 mm <sup>2</sup> and 0.785 mm <sup>2</sup> (ITBCC) at the invasive front | TBs identified on the basis of size and circularity<br>Manual correction of identified TBs   | Open-source software (IMAGE), algorithm details and code are provided              | Prediction of LNM, stratification of pT1 patients, and interobserver variability                             |
| Brieu et al. <sup>22</sup>     | 2019 | Muscle-invasive bladder cancer | 100 patients                              | Immunofluorescence | 1–4                             | Invasive front and intratumoral budding  | Deep learning to identify tumour objects<br>Machine learning for nucleus detection<br>TBs identified on the basis of the number of nuclei  | Open-source software (KERAS) for deep learning and commercial software (Definiens) | Correlation with TNM and pT staging, and proposition of new staging criteria                                 |
| Fauzi et al. <sup>15</sup>     | 2019 | CRC                            | Several patients (validated on 8 slides)  | IHC                | 1–5                             | High-power fields along the tumour border and WSI  | TBs identified on the basis of the number of nuclei and morphology   | Algorithm details are provided   | Rate of detection of individual tumour buds (sensitivity = 70%, specificity = 82%)                           |
| Brieu et al. <sup>22</sup>     | 2019 | CRC (stage II)                 | 232 patients (3 cohorts)                  | Immunofluorescence | 1–4                             | 1000-µm border inwards from the invasive front   | Manual exclusion of mucin pools and areas of necrosis<br>Machine learning for tumour object identification and segmentation<br>TBs identified on the basis of the number of nuclei | Commercial software (IndicaLabs)   | Risk model development<br>Tumour budding immune-spatial index → combined score of TB and T-cell infiltration |
| Vranes et al. <sup>19</sup>    | 2019 | Breast tumour                  | 102 patients, 532 images (~5 per patient) | IHC                | NA                              | Intratumoral   | Manual selection of ROI<br>Objects of interest identified and grouped on the basis of size and morphology  | Open-source software (IMAGE), algorithm details are provided                       | Identification of the most informative cell groups and correlation with distant metastasis occurrence        |

**Table 1.** (Continued)

| Reference                            | Year | Cancer type | Nos. of patients, slides, and images | Staining                        | TB definition (number of cells) | Investigated tissue area        | Image analysis methods  | Method availability            | Endpoints  |
|--------------------------------------|------|-------------|--------------------------------------|---------------------------------|---------------------------------|---------------------------------|---|--------------------------------|--|
| Bergler <i>et al.</i> <sup>21</sup>  | 2019 | CRC         | 87 slides                            | IHC                             | 1–4                             | Invasive front and intratumoral | Manual selection of ROI<br>Deep learning used to identify TBs on the basis of automatically selected candidates | Algorithm details are provided | TB detection (precision = 97.7%, sensitivity = 93.4%)  |
| Bokhorst <i>et al.</i> <sup>11</sup> | 2020 | CRC         | 46 patients                          | IHC (subset restained with H&E) | 1–4                             | Invasive front                  | TBs and PDCs identified on the basis of size<br>Artefacts are removed manually                                  | Algorithm details are provided | Interobserver agreement for TB identification in immunohistochemically stained slides and H&E-stained slides |

CRC, colorectal cancer; H&E, haematoxylin and eosin; IHC, immunohistochemical; ITBCC, International Tumor Budding Consensus Conference; LNM, lymph node metastasis; NA, not applicable; PDC, poorly differentiated cluster; ROI, region of interest; TB, tumour bud; TMA, tissue microarray; WSI, whole slide image.

detection can be successful without the use of machine learning.<sup>11,15,18,19</sup> For approaches that use commercially available software, the type of machine learning classifier that is used is not specified.<sup>20,23</sup> The others<sup>12,21,22,24</sup> use deep learning (one of many methods used in machine learning), more specifically convolutional neural networks, with the exception of Brieu *et al.*,<sup>22</sup> who also use random forests, which constitute an ensemble learning method based on decision trees.

Many approaches also use a two-step process: in a first step, possible budding candidates are identified on the basis of their morphology<sup>12,21</sup> or by the use of machine learning<sup>22,23</sup>; in a second step, these candidates are classified as tumour buds (versus other classes, such as background, or poorly differentiated clusters, depending on the system).

The different detection systems also use different criteria for tumour bud classification. Some use morphological features, such as the shape and size of a cluster,<sup>11,12,16–19,24</sup> whereas others identify the number of nuclei within a cluster.<sup>20,22,23</sup> These two criteria have also been combined,<sup>15</sup> and deep learning-based classification has also been implemented.<sup>12,21</sup> One study<sup>19</sup> investigated the distribution of prognostic information among malignant cell clusters according to their shape, size and count in general, without the concrete definition of a tumour bud. It was found that counting small tumor cell formations consisting of single or only several tumor cells and round clusters led to optimal prognostic performance. This type of approach is only possible with the use of computer-assisted methods, and can provide new and unique insights.

Most studies have directly used the number of identified buds or the bud grade for risk stratification, and/or correlation with survival, lymph node metastasis, and staging, without validating whether the detected objects are actually tumour buds.<sup>12,16–20,22,23</sup> Three studies, however, did evaluate the rate of recognition of the tumour buds. The best-performing system detects tumour buds in a manually selected ROI on immunohistochemically stained slides with a precision of 97.7% and a sensitivity of 93.4%.<sup>21</sup> Another study reported similar results in high-power fields on immunohistochemically stained slides but found that detection on the whole slide image remains more challenging, although there were promising results (sensitivity of 70%; specificity of 82%).<sup>15</sup>

The only system that detects tumour buds on H&E-stained slides has also shown encouraging results, with an F1 score (harmonic mean of precision and recall, maximum 100%) of 36% and a sensitivity of

72%,<sup>24</sup> but, unsurprisingly, the automated identification of tumour buds seems to be more challenging on H&E-stained slides than on immunohistochemically stained slides.

The facts that most studies have been performed on immunohistochemically stained slides and that the current guidelines for tumour bud reporting are defined on H&E-stained slides also raise the question of which cut-offs and definitions are applicable, as it is well known that tumour bud counts are significantly higher on immunohistochemically stained slides than on H&E-stained slides.<sup>11,25</sup> This issue will certainly need to be addressed before automated tumour budding can be implemented in routine practice. Only some methods are conceptually transferable to H&E-stained slides, and only two have been published so far.<sup>24</sup>

Digital systems face the same challenges as pathologists in tumour budding detection, such as distinguishing tumour buds from inflammatory cells on H&E-stained slides, or the presence of 'pseudobuds' such as cellular debris, as shown in Figure 1, or tumour cells suspended in mucin on immunohistochemically stained slides. The presence of a cell nucleus is an important criterion for tumour bud detection in order to distinguish actual buds from staining artefacts on immunohistochemically stained slides. Computer-assisted methods are better than humans at detecting differences in colour and shade intensity, which is an advantage, as overstaining decreases visibility of the nuclei.

Overall, automated detection systems have been shown to produce results that are usable for endpoint predictions and risk stratification in several cancer and staining types, as well as being able to support less experienced pathologists.<sup>17,18</sup> However, there is still much room for improvement. For instance, well-performing and thoroughly validated end-to-end solutions, which have come in the form of deep learning for many other applications, are still lacking. A possible reason for this is the need for large amounts of manually annotated data, which is a challenge in itself, as interobserver agreement at the level of an individual bud is still an issue.<sup>11</sup> A uniform method of digital scoring must also define an acceptable and reliable reference standard, which will greatly influence the output of an algorithm.

## Conclusions

Tumour budding is a very robust independent prognostic parameter that has clinical value and, according to recommendations, should be reported in

routine practice as a microscopic biomarker. Guidelines for the assessment of tumour budding represent an important step in implementing standardised reporting of tumour budding in routine practice. Further developments will undoubtedly include the automation of tumour budding detection, which may bring significant improvements in terms of time, effort, and subjectivity. Several groups have developed automated tumour budding detection algorithms, which differ significantly in terms of techniques and results. However, in order to be used in routine practice, a digital solution for tumour budding assessment will have to be validated and standardised, as has been the case for manual scoring. For this, optimal collaboration between experts in pathology and bioinformatics will be essential. Digital pathology requires considerable financial investment, and may therefore not be affordable in many parts of the world or by smaller laboratories. This issue must also be addressed if methods using digital pathology become more widespread and pragmatic cost-effective solutions are needed.

From a technical point of view, as many institutes are transitioning towards digital pathology, a semi-automated approach may be helpful. For instance, automation of ROI detection could already assist in tumour budding assessment.<sup>15,17,20,22</sup> Although digital methods face many of the same challenges as the human eye, a digital solution for scoring tumour budding is a very promising strategy, and vast improvements can be expected in the future.

## Conflicts of interest

All authors declare no conflicts of interest, including any financial, personal or other relationships with other people or organisations that could have inappropriately influenced (biased) their work.

## Author contributions

H. Dawson conceived and designed the manuscript. L. Studer, H. Dawson and A. Lugli drafted the manuscript. A. Blank contributed to the preparation of images. I. Zlobec, A. Blank, A. Fischer, I. D. Nagtegaal and J.-M. Bokhorst critically reviewed the manuscript.

## Acknowledgements

Many thanks go to Amjad Khan and Dr José Galvan for their technical assistance in preparing the images.

No funding was required for the preparation of the manuscript.

## DATA AVAILABILITY STATEMENT

Data sharing is not applicable to this article as no new data were created or analysed in this study.

## References

- Lugli A, Kirsch R, Ajioka Y *et al.* Recommendations for reporting tumor budding in colorectal cancer based on the International Tumor Budding Consensus Conference (ITBCC) 2016. *Mod. Pathol.* 2017; **30**: 1299–1311.
- Berg KB, Schaeffer DF. Tumor budding as a standardized parameter in gastrointestinal carcinomas: more than just the colon. *Mod. Pathol.* 2018; **31**: 862–872.
- Almangush A, Pirinen M, Heikkinen I, Makitie AA, Salo T, Leivo I. Tumour budding in oral squamous cell carcinoma: a meta-analysis. *Br. J. Cancer* 2018; **118**: 577–586.
- Cappellesso R, Luchini C, Veronese N *et al.* Tumor budding as a risk factor for nodal metastasis in pT1 colorectal cancers: a meta-analysis. *Hum. Pathol.* 2017; **65**: 62–70.
- Rogers AC, Winter DC, Heeney A *et al.* Systematic review and meta-analysis of the impact of tumour budding in colorectal cancer. *Br. J. Cancer* 2016; **115**: 831–840.
- Petrelli F, Pezzica E, Cabiddu M *et al.* Tumour budding and survival in stage II colorectal cancer: a systematic review and pooled analysis. *J. Gastrointest. Cancer* 2015; **46**: 212–218.
- van Wyk HC, Park J, Roxburgh C, Horgan P, Foulis A, McMillan DC. The role of tumour budding in predicting survival in patients with primary operable colorectal cancer: a systematic review. *Cancer Treat. Rev.* 2015; **41**: 151–159.
- Bosch SL, Teerenstra S, de Wilt JH, Cunningham C, Nagtegaal ID. Predicting lymph node metastasis in pT1 colorectal cancer: a systematic review of risk factors providing rationale for therapy decisions. *Endoscopy* 2013; **45**: 827–834.
- Cho SJ, Kakar S. Tumor budding in colorectal carcinoma: translating a morphologic score into clinically meaningful results. *Arch. Pathol. Lab. Med.* 2018; **142**: 952–957.
- Pagès F, Mlecnik B, Marliot F *et al.* International validation of the consensus Immunoscore for the classification of colon cancer: a prognostic and accuracy study. *Lancet* 2018; **391**: 2128–2139.
- Bokhorst JM, Blank A, Lugli A *et al.* Assessment of individual tumor buds using keratin immunohistochemistry: moderate interobserver agreement suggests a role for machine learning. *Mod. Pathol.* 2020; **33**: 825–833.
- Weis CA, Kather JN, Melchers S *et al.* Automatic evaluation of tumor budding in immunohistochemically stained colorectal carcinomas and correlation to clinical outcome. *Diagn. Pathol.* 2018; **13**: 64.
- Lino-Silva LS, Gamboa-Dominguez A, Zuniga-Tamayo D, Lopez-Correa P. Interobserver variability in colorectal cancer and the 2016 ITBCC consensus. *Mod. Pathol.* 2019; **32**: 159–160.
- Martin B, Schafer E, Jakubowicz E *et al.* Interobserver variability in the H&E-based assessment of tumor budding in pT3/4 colon cancer: does it affect the prognostic relevance? *Virchows Arch.* 2018; **473**: 189–197.



15. Fauzi MFA, Chen W, Knight D, Hampel H, Frankel WL, Gurcan MN. Tumor budding detection system in whole slide pathology images. *J. Med. Syst.* 2019; **44**: 38.
16. Pedersen NJ, Jensen DH, Lelkaitis G *et al.* Construction of a pathological risk model of occult lymph node metastases for prognostication by semi-automated image analysis of tumor budding in early-stage oral squamous cell carcinoma. *Oncotarget* 2017; **8**: 18227–18237.
17. Jepsen RK, Klarskov LL, Lippert MF *et al.* Digital image analysis of pan-cytokeratin stained tumor slides for evaluation of tumor budding in pT1/pT2 colorectal cancer: results of a feasibility study. *Pathol. Res. Pract.* 2018; **214**: 1273–1281.
18. Takamatsu M, Kawachi H, Yamamoto N *et al.* Immunohistochemical evaluation of tumor budding for stratifying T1 colorectal cancer: optimal cut-off value and a novel computer-assisted semiautomatic method. *Mod. Pathol.* 2019; **32**: 675–683.
19. Vranes V, Rajkovic N, Li X *et al.* Size and shape filtering of malignant cell clusters within breast tumors identifies scattered individual epithelial cells as the most valuable histomorphological clue in the prognosis of distant metastasis risk. *Cancers (Basel)* 2019; **11**: 1615.
20. Caie PD, Turnbull AK, Farrington SM, Oniscu A, Harrison DJ. Quantification of tumour budding, lymphatic vessel density and invasion through image analysis in colorectal cancer. *J. Transl. Med.* 2014; **12**: 156.
21. Bergler M, Benz M, Rauber D *et al.* Automatic detection of tumor buds in pan-cytokeratin stained colorectal cancer sections by a hybrid image analysis approach. In Reyes-Aldasoro CC, Janowczyk A, Veta M, Bankhead P, Sirinukunwattana K eds. *Digital Pathology*. Cham: Springer, 2019; 83–90.
22. Brieu N, Gavriel CG, Nearchou IP, Harrison DJ, Schmidt G, Caie PD. Automated tumour budding quantification by machine learning augments TNM staging in muscle-invasive bladder cancer prognosis. *Sci. Rep.* 2019; **9**: 5174.
23. Nearchou IP, Lillard K, Gavriel CG, Ueno H, Harrison DJ, Caie PD. Automated analysis of lymphocytic infiltration, tumor budding, and their spatial relationship improves prognostic accuracy in colorectal cancer. *Cancer Immunol. Res.* 2019; **7**: 609–620.
24. Bokhorst J, Rijstenberg D, Goudkade I *et al.* Nagtegaal, van der Laak J, Ciompi F. Automatic detection of tumor budding in colorectal carcinoma with deep learning. In Stoyanov D, Taylor Z, Ciompi F eds. *Computational Pathology and Ophthalmic Medical Image Analysis*. Cham: Springer, 2018; 30–138.
25. Koelzer VH, Zlobec I, Berger MD *et al.* Tumor budding in colorectal cancer revisited: results of a multicenter interobserver study. *Virchows Arch.* 2015; **466**: 485493.